AGU PUBLICATIONS

Water Resources Research

RESEARCH ARTICLE

10.1002/2013WR014485

Characteristic length scales and time-averaged transport velocities of suspended sediment in the mid-Atlantic Region, USA

James Pizzuto[1], Edward R. Schenk[2], Cliff R. Hupp[2], Allen Gellis[3], Greg Noe[2], Elyse Williamson[1], Diana L. Karwan[4], Michael O'Neal[1], Julia Marquard[5], Rolf Aalto[5], and Denis Newbold[6]

[1]Department of Geological Sciences, University of Delaware, Newark, Delaware, USA, [2]U.S. Geological Survey, Reston, Virginia, USA, [3]U.S. Geological Survey, Baltimore, Maryland, USA, [4]Department of Forest Resources, University of Minnesota, St. Paul, Minnesota, USA, [5]Department of Geography, University of Exeter, Exeter, UK, [6]Stroud Water Research Center, Avondale, Pennsylvania, USA.

Supporting Information:
- Table A1
- Supporting Figures 1–8
- Readme

Correspondence to:
J. Pizzuto,
pizzuto@udel.edu

Citation:
Pizzuto, J., et al. (2014), Characteristic length scales and time-averaged transport velocities of suspended sediment in the mid-Atlantic region, U.S.A., *Water Resour. Res.*, *50*, 790–805, doi:10.1002/2013WR014485.

Received 29 JULY 2013
Accepted 27 DEC 2013
Accepted article online 4 JAN 2014
Published online 3 FEB 2014

Abstract Watershed Best Management Practices (BMPs) are often designed to reduce loading from particle-borne contaminants, but the temporal lag between BMP implementation and improvement in receiving water quality is difficult to assess because particles are only moved downstream episodically, resting for long periods in storage between transport events. A theory is developed that describes the downstream movement of suspended sediment particles accounting for the time particles spend in storage given sediment budget data (by grain size fraction) and information on particle transit times through storage reservoirs. The theory is used to define a suspended sediment transport length scale that describes how far particles are carried during transport events, and to estimate a downstream particle velocity that includes time spent in storage. At 5 upland watersheds of the mid-Atlantic region, transport length scales for silt-clay range from 4 to 60 km, while those for sand range from 0.4 to 113 km. Mean sediment velocities for silt-clay range from 0.0072 km/yr to 0.12 km/yr, while those for sand range from 0.0008 km/yr to 0.20 km/yr, 4–6 orders of magnitude slower than the velocity of water in the channel. These results suggest lag times of 100–1000 years between BMP implementation and effectiveness in receiving waters such as the Chesapeake Bay (where BMPs are located upstream of the characteristic transport length scale). Many particles likely travel much faster than these average values, so further research is needed to determine the complete distribution of suspended sediment velocities in real watersheds.

1. Introduction

The route of suspended sediment downstream through alluvial valleys not only involves transport but also periods when particles are resting in alluvial deposits. For many rivers, the time spent resting can greatly exceed the time spent in transport. *Bradley and Tucker* [2013] suggest that "during its journey from erosional source to depositional sink, a sediment particle may spend only a small fraction of the total transit time actually moving. The remainder of the time is spent at rest, stored in various sedimentary deposits along the way." According to *Martin and Church* [2004], "sediment particles, in fact, remain at rest during most of their journey through the landscape, only rarely undergoing actual transport." *Meade* [2007] notes that "any given particle of sediment in an active river system is, at any randomly selected instant, more likely, by factors of thousands or more, to be resting quietly in storage than to be actively in motion."

Martin and Church [2004] present a useful conceptual framework for quantifying the effect of particle storage on time scales of downstream particle transport:

$$\text{travel time} = \text{travel length} / \bar{U} \tag{1}$$

The variable $\bar{U}$ in equation (1) is a "virtual velocity," the apparent (or average) rate of movement of material through the system, including the time spent in storage. If this "virtual velocity" can be determined, then the travel time for particles downstream through alluvial valleys can be estimated using equation (1).

© 2014. American Geophysical Union. All Rights Reserved.

The ability to provide travel time estimates can be critically important for watershed management. In the Chesapeake Bay watershed, for example, the EPA has set limits on sediment and phosphorus loading that states must achieve by 2025 (http://www.cbf.org.how-we-save-the-bay/chesapeake-clean-water-blueprint/what-is-killing-the-bay, accessed 5 June 2013). To reach these targets, Best Management Practices (BMPs) are employed to reduce sediment production from agricultural fields, hillslopes, eroding stream banks, and other sediment sources. Similar strategies (e.g., riparian buffers) may also be used to help reduce loading of sediment-borne contaminants or nutrients.

It is widely recognized that BMPs do not immediately improve the quality of receiving waters [*Meals et al*., 2010] because the positive sediment "signal" created by BMPs must be carried downstream through the watershed [*Meals et al*., 2010; *Hirsch et al*., 2013]. However, our ability to estimate the lag between BMP implementation and its beneficial effect on downstream receiving waters is very poorly developed. In the Chesapeake Bay Program, for example, BMPs are evaluated using the Chesapeake Bay Model (www.chesapeakebay.net/about/programs/modeling/53/, accessed 10 July 2013), a version of the hydrologic model HSPF. While the Chesapeake Bay Model is a very advanced watershed simulation model, it routes sediment downstream along with channelized flow without considering off-channel sediment storage and exchange processes, and it therefore cannot assess sediment lag times.

Fluvial geomorphologists and engineers have developed several methods in recent years for predicting the transport and storage of sediment (and attached contaminants) in alluvial systems. Over short spatial and temporal scales, 2-D and 3-D hydrodynamic models can be used to assess patterns and rates of sediment transport, storage, and remobilization [*Crosato and Saleh*, 2011; *Warwick and Carroll*, 2008]. Reduced complexity models have been developed to route sediment-borne contaminants through watersheds [*Coulthard and Macklin*, 2003]. Markov models use observed sediment budget data to estimate the probability of sediment "transitions" from one alluvial storage reservoir into another, thereby quantifying the various paths and rates of downstream sediment movement [*Kelsey et al*., 1987; *Malmon et al*., 2002]. Several recent 1-D reach-averaged models couple equations for hydraulics, sediment transport, erosion, and deposition, and these models can be used to estimate the downstream movement and storage of sediment, contaminants, and associated isotopes [*Lauer and Parker*, 2008a, 2008b, 2008c; *Lauer and Willenbring*, 2010; *Viparelli et al*., 2013].

All of these methods are significant contributions, but each has important disadvantages. Detailed hydrodynamic models can only represent short time and spatial scales, while the watershed routing problem may encompass thousands of kilometers of river channels and millennial time scales. The reduced complexity models can be applied at the appropriate temporal and spatial scales, but they may fail to capture the specific controlling processes of transport and exchange. Markov models require alluvial storage reservoirs to be well-mixed, but this assumption may not be reasonable [*Ackerman and Pizzuto*, 2012; *Bradley and Tucker*, 2013].

The reach-averaged hydraulic routing models could likely be adapted to achieve the objectives of our research, but here we choose a more straightforward approach. We assume that sediment budget components are known, and we use mass conservation principles to derive a theoretical framework allowing sediment budget data to be related to the downstream movement of "tagged" suspended sediment particles as a function of downstream distance and time. The resulting equations are valid for temporally and spatially varying sediment budget components (though the budget must be specified; it is not predicted by the theory), and they also account for grain size partitioning between the channel and floodplain (for example, if coarse-grained sediment is preferentially deposited and fine-grained sediment is preferentially transported). A simple scaling analysis derived from our theory identifies a characteristic length scale, L_s, that represents the distance particles are carried in transport before they enter storage.

The virtual velocity $\bar{U}$ in equation (1) can be represented as the ratio of a length scale to a characteristic time scale. We propose that the appropriate length scale for estimating $\bar{U}$ is the characteristic transport length L_s, and that the appropriate time scale is T_f, the average time particles spend in storage before being remobilized. This hypothesis implies that the time particles spend in transport may be entirely neglected: only the storage time is necessary to estimate $\bar{U}$. We document, as part of our analysis, the conditions required for this hypothesis to be a reasonable approximation.

These results and equation (1) lead us to develop a conceptual model for the lag time of suspended sediment signals influenced by storage, and to hypothesize that lag times in the mid-Atlantic region are

© 2014. American Geophysical Union. All Rights Reserved.

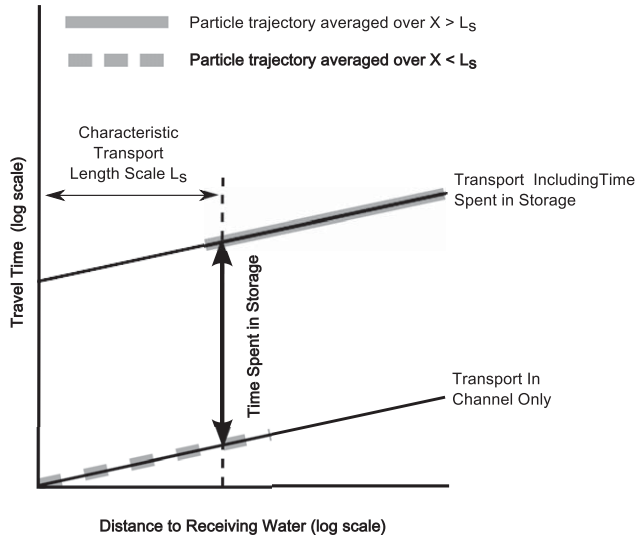

Figure 1. Conceptual illustration (on log-log axes) of the influence of particle storage on travel time of a representative suspended sediment particle to receiving waters downstream. For transport distances less than L_s, most particles remain in the channel and are carried rapidly downstream with the flow. After a distance L_s, most particles have entered storage, and travel times reflect the additional time spent "resting" in storage.

increased by orders of magnitude where storage in floodplains is important. The conceptual model posits that, for transport distances significantly shorter than L_s, suspended particles are primarily transported with the water in the channel, and travel times to receiving waters are relatively short (Figure 1). After particles are carried farther than L_s, nearly all will have been deposited and stored, and their subsequent movement must proceed at a lower velocity that includes the time spent in storage. As a result, travel times will be considerably longer (Figure 1). The primary goal of the analysis that follows is to present a quantitative version of Figure 1 using data from the mid-Atlantic region.

2. Study Areas and Selected Methods of Data Analysis

Although the theory presented in this paper is very general, it is used here to estimate spatial and temporal scales of suspended sediment routing for mid-Atlantic upland streams (i.e., sites located in the Coastal Plain are excluded) [*Bachman et al.*, 1998]. Four of our five study sites are tributaries of the Chesapeake Bay, while one is a tributary of the Delaware Bay.

Data are obtained from U.S. Geological Survey gaging stations and sediment budget analyses (Figure 2). Field and analytical methods are mostly presented in the original publications. Methods used to cast data into a form useful for the purposes of this paper are briefly described here.

2.1. Sediment Budget Information From Previous Studies

Hupp et al. [2013] and *Schenk et al.* [2013] present sediment budgets for three watersheds with drainage basin areas of 141 km^2 (Difficult Run), 147 km^2 (Linganore Creek), and 160 km^2 (Little Conestoga River) (Figure 2). Floodplain deposition rates were measured using clay pads as reference horizons, and bank erosion rates were determined using erosion pins. Sediment yields [reported by *Schenk et al.*, 2013] are estimated from U.S. Geological Survey gaging stations in each watershed. Data for these studies were collected over a relatively short period of a few years. The percentages of silt-clay and sand in floodplain deposits ($n = 36$, 18, and 19 samples from Difficult Run, Linganore Creek, and the Little Conestoga River) were measured using a sonic sifter (Linganore Cr, and Little Conestoga River) or a LISST (Sequioa Scientific, Inc) (Difficult Run) (grain size data have not been previously published). The percentages of silt-clay and sand in suspended sediment samples were obtained from gaging station data available in the U. S. Geological Survey's National Water Information

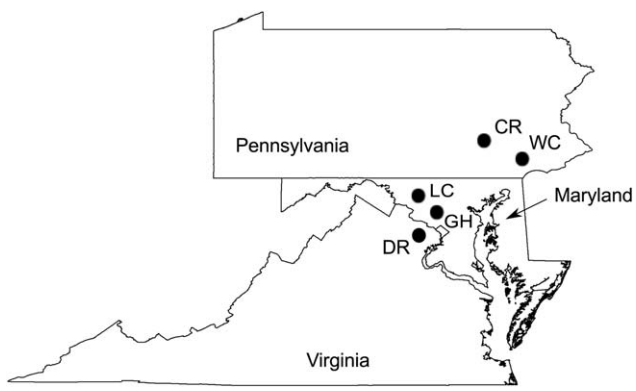

Figure 2. Locations of sites where data are reported in this paper. CR—Little Conestoga River; DR—Difficult Run; GH—Good Hope Tributary; LC—Linganore Creek; and WC—White Clay Creek at Stroud Water Research Center.

© 2014. American Geophysical Union. All Rights Reserved.

Table 1. Data Used to Determine the Percentage of Silt-Clay and Sand in Suspended Sediment Samples

Drainage Basin	Sampling Sites	U.S. Geological Survey Gaging Station ID #	Number of Samples	Sampling Period
Good Hope Tributary, MD	Seven sites in Rock Cr. and Anacostia R. basins[a]	NA	58	9/12/1960–12/26/1973
White Clay Creek (WCC), PA	WCC at Stroud Water Research Center	NA	27	6/24/2011–10/31/2012
Linganore Creek (LC), MD	LC near Libertytown, MD	01642438	458	9/6/2008–1/4/2011
Little Conestoga Cr (LCC), PA	LCC, Site 3A, near Morgantown, PA, and LCC near Churchtown, PA	0157608335 and 01576085	110	3/21/1983–7/24/1988
Difficult Run (DR), VA	DR near Great Falls, VA	01646000	39	7/13/2011–5/16/2013

[a]Data summarized by *Yorke and Herb* [1978].

System (http://nwis.waterdata.usgs.gov/usa/nwis/qwdata, accessed 25 June 2013) (Table 1). Individual estimates were weighted by suspended sediment flux at the time of sampling to obtain a representative flux-weighted mean % silt-clay and sand for each gaging station.

Williamson [2013] created a sediment budget for sand and silt-clay grain size fractions for a 0.725 km-long section of the third-order White Clay Creek near the Stroud Water Research Center (SWRC) (http://www.stroudcenter.org/, accessed 12 June 2013). She measured erosion and deposition rates associated with lateral channel migration (deposition from overbank flows was neglected) from historical (1968 and 2010) aerial imagery and high-resolution light detection and range (LIDAR) data using methods described by *Rhoades et al*. [2009]. Six channel samples of eroding banks were obtained and the percentages of silt-clay and sand determined by wet-sieving [*Lewis*, 1984]. The annual average suspended sediment yield was estimated from 18 years of gaging station data collected at the SWRC. *Williamson* [2013] first created a sediment rating curve and developed a procedure to correct for statistical bias [e.g., *Ferguson*, 1986]. The rating curve was used to estimate suspended sediment transport rates associated with each discharge measurement (obtained at either 15 or 5 min intervals) in the 18 year database; these individual loads were summed to determine annual loads. The percentages of silt-clay and sand in suspended sediment were measured from 27 samples obtained over a wide range in discharge from 2010 to 2012 (Table 1). The grain size of these samples was measured using a Micromeritics S100 SediGraph at the University of Exeter. Similar to the data obtained from the U.S. Geological Survey, individual grain size estimates for suspended sediment were weighted by suspended sediment flux at the time of sampling.

Allmendinger et al. [2007] developed a sediment budget for the Good Hope Tributary (drainage basin area 4.05 km^2) for 1951–1996. Floodplain deposition was measured using dendrochronological methods, and statistical relationships were used to estimate upland sediment production and bank erosion. Sediment yield was not measured directly, but was rather obtained by summing the individual budget components (i.e., the output was given as the sum of inputs minus storage components). While *Allmendinger et al*. [2007] do not present grain size data for budget components, a complete sediment budget by grain size fraction is presented by *Allmendinger* [2004]. To estimate the fractions of silt-clay and sand in the suspended sediment load, 58 analyses from other nearby watersheds presented by *Yorke and Herb* [1978] are used (Table 1). These data were averaged without weighting grain size estimates by suspended sediment flux, because they were obtained from several different sites.

Sediment budget data are primarily used in this paper to estimate the intensity of sediment exchange relative to the suspended sediment transport rate; the balance between erosion and deposition is not particularly important. Furthermore, the large errors associated with sediment budget estimates often preclude clear assessment of the sediment balance, as the balance is typically a small difference between large numbers, each of which has significant error. Accordingly, for all sites except the White Clay Creek, estimates of erosion and deposition are averaged here to obtain a single estimate of sediment exchange, essentially assuming that the mass of floodplain sediment storage is constant. At the White Clay Creek, rates of overbank deposition have not been measured, and so a somewhat different approach is needed. We assume that the unmeasured accumulation would increase sediment storage to approximately balance erosion, and therefore we use the bank erosion rate for the White Clay Creek to estimate sediment exchange at this

© 2014. American Geophysical Union. All Rights Reserved.

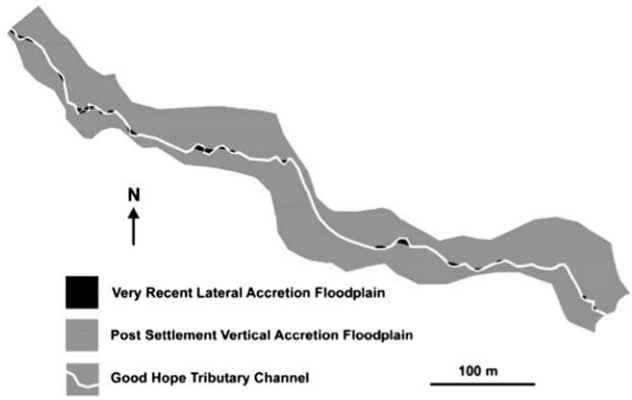

Figure 3. Geomorphic map illustrating the areal extent of fine-grained postsettlement vertical accretion floodplain deposits and coarse-grained very recent lateral accretion deposits of the Good Hope Tributary, Maryland. Nearly all the banks composed (J. Pizzuto, unpublished data, 2004) of postsettlement vertical accretion deposits are eroding.

site. Clearly, all of these methods represent rather crude approximations (particularly so for the White Clay Creek). However, since the goal of this paper is to estimate generalized scaling parameters, and not to produce detailed model results, our approach (though approximate) is appropriate.

2.2. Stratigraphy and Holocene-Recent Depositional History of Upland Mid-Atlantic Rivers

The texture and stratigraphy of alluvial deposits has an important influence on the intensity of exchange between storage reservoirs and suspended sediment transported in the channel. For example, if most of the sediment eroded from storage is coarse-grained bed material, the intensity of exchange of fine-grained suspended sediment will be diminished, and the transport distance L_s will increase. *Lauer and Parker* [2008c], for example, assumed that eroding banks in meandering streams are composed a thick underlying deposit of coarse-grained point bar sediments overlain by a thin deposit of fine grained overbank sediments. This stratigraphic model (applied to eight sites along three meandering rivers) resulted in estimated characteristic length scales (L_s) of 7.3–54 km for sandy point bar sediments and 106–27,300 km for silt and clay overbank sediments.

Stratigraphic studies of mid-Atlantic floodplains describe deposits that are dramatically different from those associated with meandering streams [*Jacobson and Coleman*, 1986; *Pizzuto*, 1987; *Walter and Merritts*, 2008]. Prior to European settlement, many mid-Atlantic floodplain deposits consisted of a thin (~few decimeters) basal layer of gravel overlain by less than 1 m of fine-grained, locally organic-rich silt and clay deposits that is occasionally capped by a well-developed buried A horizon [*Jacobson and Coleman*, 1986; *Pizzuto*, 1987]. After European settlement, valleys alluviated rapidly as a result of soil erosion [*Happ et al.*, 1940; *Trimble*, 1971; *Jacobson and Coleman*, 1986] and mill dam construction [*Walter and Merritts*, 2008], burying the presettlement floodplains with several meters of silty overbank deposits. In the 20th Century, these fine-grained floodplains began to be reworked by slow lateral migration of ~0.1 m/yr [*Allmendinger et al.*, 2005; *Pizzuto and Meckelnburg*, 1989; *Rhoades et al.*, 2009], while accretion of overbank deposits on the valley flat continues (at least locally) at diminished rates [*Allmendinger et al.*, 2007; *Bain and Brush*, 2005; *Hupp et al.*, 2013; *Schenk et al.*, 2013; *Smith*, 2011].

As a result of this history, alluvial deposits of the mid-Atlantic region are typically dominated by fine-grained vertical accretion deposits (Figure 3) [*Pizzuto*, 1987; *Jacobson and Coleman*, 1986; *Walter and Merritts*, 2008; *Hupp et al.*, 2013; *Jackson et al.*, 2005], while coarser-grained lateral accretion deposits are poorly developed (and they only occur in small units adjacent to the channel that are inset into, rather than underlying, the fine-grained valley fill). Eroding cutbanks, therefore, consist predominantly of fine-grained sediment that can travel in suspension, suggesting that sediment eroded from storage reservoirs is mostly fine grained (Figure 4). Furthermore, rates of lateral migration and vertical accretion are slow enough that the morphology of alluvial landforms appears approximately static on decadal (and even centennial) time scales [*Rhoades et al.*, 2009], unlike the laterally migrating systems considered in other recent models of fine-grained sediment routing [*Viparelli et al.*, 2013; *Lauer and Parker*, 2008a, 2008b, 2008c].

2.3. Estimating Sediment Transit Times for Mid-Atlantic Floodplains

The time particles spend in storage, or their "transit time" (in the terminology of reservoir theory) [*Bolin and Rhode*, 1973], is an important variable in the theory presented here. While a rigorous estimate of particle transit time is difficult to achieve, *Lancaster and Casebeer* [2007] and *Lancaster et al.* [2010] suggest that the

© 2014. American Geophysical Union. All Rights Reserved.

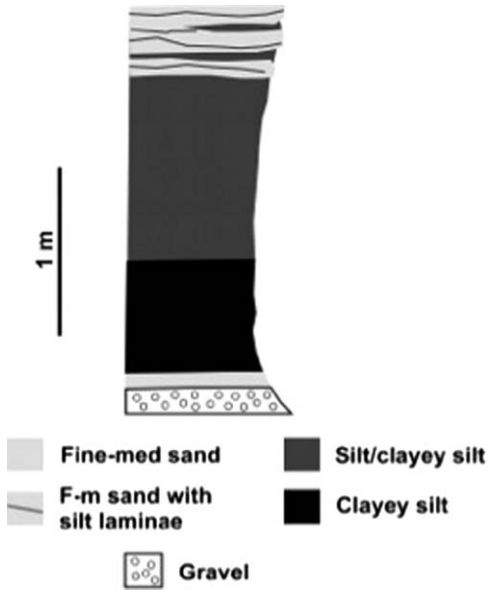

Figure 4. Typical cutbank stratigraphy of mid-Atlantic upland streams [redrawn from *Jacobson and Coleman*, 1986]. The contact between the underlying clayey silt and the overlying silt/clayey silt represents the boundary between presettlement and postsettlement deposits.

age distribution of eroding banks can be used as a reasonable estimate for the transit time distribution of particles in storage.

Data for this approach are also fairly meager. Here, we estimate the age distribution of the vertical sequence illustrated in Figure 4, because most eroding banks are removing these sediments (as documented in Figure 3). Fifty-seven published radiocarbon dates from the mid-Atlantic region document the ages of the presettlement deposits illustrated in Figures 3 and 4. Many of these (but not all) are obtained from eroding banks, simply because these exposures are the easiest place to obtain samples for dating. Dates for the postsettlement deposits of the mid-Atlantic region are relatively rare, and most of these are from cores rather than eroding banks [e.g., *Bain and Brush*, 2005], so few useful ages for postsettlement eroding bank deposits are available.

A very approximate mean transit time for mid-Atlantic floodplains is estimated for the geometry of the deposits in Figure 4, an average age for presettlement deposits, an estimate of the date of the contact between presettlement and postsettlement units, and an assumed constant sedimentation rate of postsettlement deposits. The average age of presettlement deposits is estimated by simply averaging the radiocarbon dates from this unit. The date of European settlement is taken to be 1750 [*Jacobson and Coleman*, 1986; *Walter and Merritts*, 2008], and sedimentation from 1750 to the present is assumed to have proceeded at a constant rate (though likely not precisely correct, this assumption does not materially influence the "order of magnitude" results presented here). Finally, we assume that Figure 4 depicts typical values for the thickness of presettlement and postsettlement deposits. Based on these assumptions, the mean age $\bar{A}$, of sediments eroded from lateral migration is

$$\bar{A} = \frac{T_{\text{pre-S}}}{T}\bar{A}_{\text{pre-S}} + \frac{T_{\text{post-S}}}{T}\bar{A}_{\text{post-S}} \tag{2}$$

where T is the total height of the eroding bank, and the subscripts "pre-S" and "post-S" refer to presettlement and postsettlement deposits. The average age of the postsettlement deposits, $\bar{A}_{\text{post-S}}$, is computed as (2000–1750)/2, or 125 years. From Figure 4, $T_{\text{pre-S}}$ and $T_{\text{post-S}}$ are assigned values of 0.5 m and 1.75 m, respectively.

3. Theory

A mass balance approach is followed here to derive equations describing the downstream movement of "tagged" suspended sediment affected by sediment storage outside the stream channel. Suspended sediment may become "tagged" by introducing a contaminant that sorbs strongly to sediment; in this case, the theory predicts the concentration of the contaminant on the sediment that is moving downstream. The theory, however, also applies in the absence of a contaminant or identifiable tracer. In this case, the "tagging" may simply indicate a specific population of sediment that is to be followed downstream. *Lauer and Parker* [2008a] use a

© 2014. American Geophysical Union. All Rights Reserved.

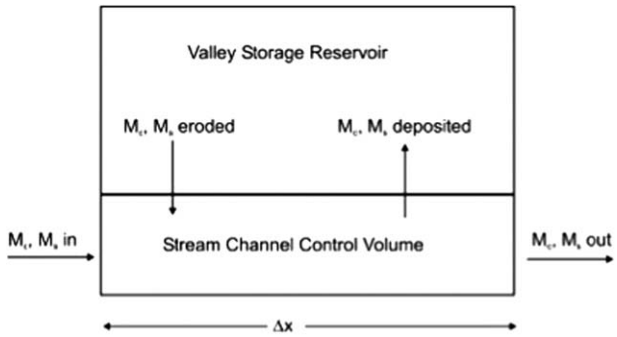

Figure 5. Control volume for deriving mass balance equations for sediment and "contaminated" or tagged sediment particles. Terms indicated by "M" have units of mass; subscripts "*s*" and "*c*" refer to sediment and contaminant, respectively.

similar terminology and approach; *Doyle and Ensign* [2009] outline the considerable utility for a conceptual framework that allows a population of tagged sediment to be "followed" on its path through a river network.

A river valley segment of length Δx (on the order of a kilometer) is divided into two separate domains, a channel control volume and an adjacent alluvial storage reservoir (Figure 5). The channel control volume consists of the water (and sediment) in the stream channel and is defined by the wetted perimeter and water surface boundaries of the stream. The alluvial storage reservoir consists of all the deposits of the river valley that store suspended sediment (separate storage reservoirs could easily be defined and treated with separate mass balance equations, but this would unnecessarily complicate the analysis).

Suspended sediment transport is highly episodic, and may only be significant during infrequent storm events. Following *Paola et al*. [1992] and *Parker and Cui* [1998], elapsed time is divided into two binary states, one when transport is significant, denoted t^*, and another when no transport occurs. The duration of a transport event is denoted as Δt^*, such that the fraction of time composed of transport events, I, is $\Delta t^*/\Delta t$, where Δt is a useful time step for sediment budgeting (such as a year).

This study is based on the hypothesis that time spent in storage greatly reduces the downstream transport velocity of suspended particles (as summarized by Figure 1). One consequence of this idea is that the magnitude and frequency of storm events is unlikely to strongly influence downstream transport time scales for length scales that exceed L_s (if storage time scales are indeed as long as schematically depicted in Figure 1). Accordingly, transport events are represented as being of constant magnitude, frequency, and duration here. Specifically, the downstream velocity during "events" is set equal to a constant value of 1 m/s, and the fraction of time composed of transport events is set equal to 0.01, both reasonable values for the velocity of bankfull discharges and for the recurrence interval of dominant sediment transporting events [*Guy*, 1964].

3.1. Sediment Mass Balance Equation

The first step in developing the theory is to express the mass balance of a single grain size fraction, such as silt-clay, during a transport (storm) event:

$$\frac{\partial(M_s p_c)}{\partial t^*} = -\frac{\partial(\rho_w Q C_s p_c)}{\partial x}\Delta x + \frac{M_{seroded} p_F}{\Delta t} - \frac{M_{sdep} p_F}{\Delta t} \tag{3}$$

where M_s is the mass of suspended sediment stored in the water column of the reach, p_c is the fraction of total suspended sediment in the channel composed of silt-clay (or any other grain size fraction of interest), Q is the water discharge, ρ_w is the density of water, C_s is the mass concentration suspended sediment in the water column (including all size fractions), p_F is the fraction of stored sediment composed of silt and clay, and $M_{seroded}$ and M_{sdep} are the masses of sediment removed from storage (through erosion) and entering storage (through deposition) during a time period Δt.

The mass of suspended sediment in the reach, M_s can be written as $\rho_w WH\,\Delta x C_s$, where W and H are the width and depth of the flow, respectively. Substituting this quantity into the left side of equation (3), treating the water density as a constant, noting that the length of the reach is independent of time, and rearranging leads to

© 2014. American Geophysical Union. All Rights Reserved.

$$\frac{\partial(WHC_s p_c)}{\partial t^*} = -\frac{\partial(QC_s p_c)}{\partial x}\Delta x + \frac{M_{seroded} p_F}{\Delta x \Delta t \rho_w} - \frac{M_{sdep} p_F}{\Delta x \Delta t \rho_w} \tag{4}$$

Sediment erosion (F_e) and deposition (F_d) rates per unit channel length and time that include all grain size fractions are defined and substituted into equation (4)

$$\frac{\partial(WHC_s p_c)}{\partial t^*} = -\frac{\partial(QC_s p_c)}{\partial x} + \frac{F_e p_F}{\rho_w} - \frac{F_d p_F}{\rho_w} \tag{5}$$

Accounting for intermittency of transport such that $t^* = It$ leads to

$$\frac{\partial(WHC_s p_c)}{\partial t} = -I\frac{\partial(QC_s p_c)}{\partial x} + \frac{IF_e p_F}{\rho_w} - \frac{IF_d p_F}{\rho_w} \tag{6}$$

Equation (6), which expresses the mass conservation of suspended sediment in the channel, is not directly used in this paper. However, it is necessary to express the equation for "tagged" suspended sediment conservation in a compact form.

3.2. Conservation Equation for Contaminated ("Tagged") Sediment

The mass balance for contaminated suspended sediment can be derived using similar arguments to those used for sediment, but to obtain the mass of contaminant, the sediment mass must be multiplied by the mass concentration of the contaminant in each budget component, which will be denoted C_{Hg}. This leads to

$$\frac{\partial(M_s p_c C_{Hgc})}{\partial t^*} = -\frac{\partial(\rho_w QC_s C_{Hgc} p_c)}{\partial x}\Delta x + \frac{M_{seroded} p_F C_{HgF}}{\Delta t} - \frac{M_{sdep} p_c C_{Hgc}}{\Delta t} \tag{7}$$

where as above, the subscript "c" refers to conditions in the channel and the subscript "F" denotes the average concentration of the contaminant in sediment eroded into the channel from storage.

Relying on previous definitions for the mass of sediment in suspension and using previously defined quantities F_e, F_d, and accounting for intermittent events leads to

$$\frac{\partial(WHC_s C_{Hgc} p_c)}{\partial t} = -I\frac{\partial(QC_s C_{Hgc} p_c)}{\partial x} + \frac{IF_e p_F C_{HgF}}{\rho_w} - \frac{IF_d p_c C_{Hgc}}{\rho_w} \tag{8}$$

Partial derivatives in time t and position x in equation (8) are now expanded

$$\frac{\partial(WHC_s C_{Hgc} p_c)}{\partial t} = C_{Hgc}\frac{\partial(WHC_s p_c)}{\partial t} + WHC_s p_c \frac{\partial(C_{Hgc})}{\partial t} \tag{9}$$

$$\frac{\partial(QC_s C_{Hgc} p_c)}{\partial x} = C_{Hgc}\frac{\partial(QC_s p_c)}{\partial x} + QC_s p_c \frac{\partial(C_{Hgc})}{\partial x} \tag{10}$$

Equations (9) and (10) are substituted into equation (8), and the sediment continuity equation (6) is substituted for the first term on the right of equation (9). After some reorganization, equation (11) is obtained

$$\frac{\partial C_{Hgc}}{\partial t} = -\frac{IQ}{WH}\frac{\partial C_{Hgc}}{\partial x} + \frac{IF_e p_F (C_{HgF} - C_{Hgc})}{\rho_w WHC_s p_c} \tag{11}$$

The quantity Q/WH is the definition of U, the mean velocity of flow during an event. Similarly, $\rho_w WHC_s U$ is the mass flux of suspended sediment. This motivates defining f_e as the fraction of the total suspended sediment load supplied to the channel per unit channel length by erosion of material from storage, leading to

© 2014. American Geophysical Union. All Rights Reserved.

$$\frac{\partial C_{Hgc}}{\partial t} = -IU\frac{\partial C_{Hgc}}{\partial x} + IUf_e\frac{p_F}{p_c}(C_{HgF} - C_{Hgc}) \tag{12}$$

The mean velocity U refers to the movement of water during transport events. When multiplied by I, the quantity IU is the velocity of the water averaged over both transport and nontransport events. Defining IU as the quantity $\hat{U}$

$$\frac{\partial C_{Hgc}}{\partial t} = -\hat{U}\frac{\partial C_{Hgc}}{\partial x} + \hat{U}f_e\frac{p_F}{p_c}(C_{HgF} - C_{Hgc}) \tag{13}$$

Equation (13) is valid for a variety of conditions, including spatially and temporally varying sediment exchange with storage (i.e., f_e can vary with both space and time). Floodplain and channel grain size fractions p_F and p_C can also vary with both space and time. It might appear that equation (13) totally ignores the process of sediment deposition, but this is not the case: changing sediment deposition will change the flux of suspended sediment through the reach, thereby changing the value of f_e. Of course, to actually account for these complexities, the sediment continuity equation must be explicitly solved in addition to equation (13) (otherwise, the value of f_e will not be known). In this paper, however, spatial and temporally varying parameters are not accounted for, so these issues are not of concern.

Equation (13) is a kinematic wave equation with an added "source/sink" term. The first term on the right represents wavelike movement of contaminated sediment downstream at a rate of $\hat{U}$, while the second term represents changes in concentration that arise from exchange of contaminated sediment with storage reservoirs. The reservoir exchange term will initially reduce the rate of downstream transport of contaminant, because it is negative when contaminated sediment first enters a reach, and the floodplain has yet to be contaminated. The floodplain can switch from a sink to source if floodplain contaminant concentration $C_{Hg\ F}$ exceeds channel concentration $C_{Hg\ c}$.

Equation (13) also illustrates the importance of grain size partitioning between the channel and the floodplain. The reservoir exchange term on the far right depends on the quantity $f_e p_F/p_c$. Exchange is enhanced (and the downstream transport of contaminant is reduced) when the rate of erosion per unit length (f_e) is high. However, if silt and clay are preferentially transported rather than deposited, such that $p_F < p_C$, then the importance of exchange is reduced. Thus, the tendency for fine-grained sediment to be transported rather than stored can counteract the influence of storage in reducing the downstream transport velocity of contaminated sediment.

3.3. Characteristic Length Scale (L_s) For Downstream Transport Without Storage

Rather than actually presenting a solution to equation (13), a characteristic length scale is derived from it that represents how far particles are typically transported without being stored (and whose downstream velocity along this path is $\hat{U}$) [see *Lauer and Parker*, 2008a, 2008c, for similar analyses]. Consider a uniform channel without tributaries. All parameters in equation (13) are constant over space and time. Initially, none of the sediments are tagged with a contaminant. Then, a mass of contaminant is instantaneously introduced, creating an initial concentration C_{Hgc0} at $x = 0$. If an observer moves downstream along with the contaminant at a velocity $\hat{U}$, the observer will travel a distance $s = \hat{U}t$. The contaminant concentration seen by this observer will gradually decrease, because the contaminated sediments are continually being deposited and replaced by sediment from storage that has not yet been contaminated (i.e., $C_{Hg\ F}$ is 0 at $s = \hat{U}t$). The concentration seen by the observer decreases exponentially according to equation (14):

$$C_{Hgc} = C_{Hgc0}e^{-f_e p_F s/p_c} = C_{Hgc0}e^{-s/L} \tag{14}$$

Equation (14) suggests that the characteristic length scale for "channel transport" without storage, L_s, is

$$L_s = \frac{p_c}{p_F f_e} \tag{15}$$

After a transport distance of L_s, the concentration $C_{Hg\ c}$ has decreased to 1/e (37%) of its initial value, because 63% of the initial contaminant mass has been exchanged with uncontaminated sediment removed from storage. The channel transport distance L_s decreases with increasing exchange intensity f_e. If fine-

© 2014. American Geophysical Union. All Rights Reserved.

grained sediment is preferentially transported rather than stored (i.e., if $p_c > p_F$), then the channel transport distance L_s will also increase. *Lauer and Willenbring* [2010, equation (15e)] and *Lauer and Parker* [2008c, equation (32)] have derived length-scale equations that are essentially equivalent to equation (15).

3.4. Suspended Sediment Transport Velocity Averaged Over Storage Time Periods

Figure 1 illustrates the consequences of storage on the downstream travel time of suspended sediment particles. In order to quantify this concept, an equation is needed for the transport velocity averaged over time periods spent in storage. To simplify the analysis, the sediment budget components and fractions of silt-clay in the channel and floodplain are assumed to be constant with time, even though more general expressions can be readily derived.

The time-averaged downstream velocity for silt-clay (results for sand simply require a change of subscripts) averaged over storage periods, $\bar{U}_{\text{silt-clay}}$ can be written as

$$\bar{U}_{\text{silt-clay}} = \frac{\Delta x}{\bar{A}_{\text{silt-cay}}} \tag{16}$$

where $\bar{A}_{\text{silt-clay}}$ is the average elapsed time a silt-clay particle spends in the reach of length Δx (i.e., $\bar{A}_{\text{silt-clay}}$ is the average transit time for particles leaving the reach).

The quantity $\bar{A}_{\text{silt-clay}}$ can be divided into two components, one composed of sediment that traverses the reach without entering storage, and the other composed of sediment removed from storage within the reach that subsequently exits the reach in suspension. $\bar{A}_{\text{silt-clay}}$ is then the sum of the characteristic transit times for each component, weighted by the fraction of the total suspended sediment load that comprises each component:

$$\bar{A}_{\text{silt-clay}} = (1 - F_F)\bar{A}_c + F_F\bar{A}_F \tag{17}$$

where F_F is the fraction of the suspended silt-clay leaving the reach that was removed from storage within the reach, $\bar{A}_c$ is the average transit time for particles carried in suspension through the reach without spending time in storage, and $\bar{A}_F$ is the average transit time for particles leaving the reach that spent time in storage within the reach.

The quantity F_F can be readily expressed in terms of previously defined variables

$$F_F = \frac{F_e p_F \Delta x}{\rho_w Q C_s p_c} = \frac{f_e p_F \Delta x}{p_c} \tag{18}$$

Noting that the average transit time of particles carried through the reach in the channel is simply $\Delta x/\hat{U}$, substituting this result and equation (18) into equation (17), and rearranging leads to

$$\bar{U}_{\text{silt-clay}} = \frac{1}{\frac{1}{\hat{U}}\left(1 - \frac{f_e \Delta x p_F}{p_c}\right) + \frac{f_e p_F}{p_c}\bar{A}_F} = \frac{1}{\frac{1}{\hat{U}}\left(1 - \frac{\Delta x}{L_s}\right) + \frac{\bar{A}_F}{L_s}} \tag{19}$$

Note that where no sediment is supplied from storage (i.e., $f_e = 0$), $\bar{U}_{\text{silt-clay}} = \hat{U}$. Storage will control the rate of downstream sediment movement when the following conditions apply:

$$\frac{1}{\hat{U}}\left(1 - \frac{\Delta x}{L_s}\right) \ll \frac{\bar{A}_F}{L_s} \tag{20}$$

$$\frac{L_s}{\hat{U}}\left(1 - \frac{\Delta x}{L_s}\right) \ll \bar{A}_F \tag{21}$$

i.e., when the time spent in storage $\bar{A}_F$ is much greater than the travel time of a particle $L_s/\hat{U}$ within the water column over the length scale L_s (assuming that the quantity in parentheses $\sim$1). When equation (21) is satisfied, then equation (19) is closely approximated as

© 2014. American Geophysical Union. All Rights Reserved.

Table 2. Sediment Budget Data and Suspended Sediment Transport Length Scales and Time-Averaged Velocity Values Derived From the Sediment Budget Data[a]

	Site				
Variable	Good Hope Tributary[b]	White Clay Creek	Linganore Cr	Little Conestoga Cr	Difficult Run
Drainage Basin Area (km^2)	4.05	7.25	147	160	163.9
Floodplain Sedimentation	4000 (2000) (m^3)	29 (Mg/yr)[c]	1090 (Mg/yr)	4300 (2800) (Mg/yr)	13,900 (13,000) (Mg/yr)
Bank Erosion	3200 (800) (m^3)	47 (Mg/yr)	1020 (820) (Mg/yr)	3670 (2560) (Mg/yr)	1470 (2740) (Mg/yr)
Mean Exchange[d]	3600 (2150) (m^3)	47 (Mg/yr)[e]	1050 (820) (Mg/yr)	4000 (1900) (Mg/yr)	7700 (4600) (Mg/yr)
Sediment Flux	8100 (4200) (m^3)	360 (77) (Mg/yr)	6390 (Mg/yr)	10,420 (Mg/yr)	23,100 (Mg/yr)
Reach Length (km)	1	0.725	7.9	24.4	19
Mean Exchange/km/Flux	0.44 (0.35)	0.18 (0.04)	0.020 (0.016)	0.016 (0.008)	0.018 (0.011)
p_F[f] (silt-clay)	52 (21)	38 (11)	82	93	75
p_c (silt-clay)	80 (11)	96 (13)	83 (14)	89 (13)	70 (24)
p_F[f] (sand)	48 (21)	62 (15)	18 (10)	7 (3)	25 (16)
p_c (sand)	20 (21)	4.3 (4.3)	18	11	31
L_s (silt-clay)	4 (2)	14 (6)	48 (37)	60 (31)	52(36)
L_s (sand)	1 (1)	0.4 (0.4)	46 (44)	113 (75)	68 (60.0)
Time-averaged velocity (km/yr) (silt-clay)	0.0072	0.029	0.098	0.12	0.11
Time-averaged velocity (km/yr) (sand)	0.0019	0.00080	0.095	0.20	0.14

[a]Values in parentheses are standard deviations based on variability of individual measurements (data not available if missing).
[b]All values are totals for the period 1951–1996.
[c]From lateral migration only (overbank deposition not included).
[d]Average of floodplain sedimentation and bank erosion (except for White Clay Creek).
[e]Bank erosion used here because overbank deposition was not measured.
[f]Floodplain % sand and % silt-clay measured on eroding banks.

$$\bar{U}_{\text{silt-clay}} = \frac{L_s}{\bar{A}_F} = \frac{p_c}{\bar{A}_F p_F f_e} \tag{22}$$

Equation (22) is identical to the hypothesis presented in section 1. This analysis clarifies the conditions required for this hypothesis to be valid.

4. Results

4.1. Sediment Budget Data and Suspended Sediment Transport Length Scales

The fraction of the annual suspended sediment flux exchanged from storage per kilometer (f_e) for the five study areas ranges from a minimum of 0.016 (Little Conestoga Cr.) to a maximum of 0.44 (Good Hope Tributary) (Table 2). Values of f_e tend to decrease with increasing drainage basin area, suggesting that the rate of increase in sediment flux with drainage basin area exceeds the rate of increase in exchange with drainage basin area.

There are no consistent differences between the % silt-clay carried in suspension (p_c (silt-clay) in Table 2) and the % silt-clay of eroding bank sediments (p_F (silt-clay) in Table 2). At three of the sites, p_c exceeds p_F, while at two of the sites, p_F exceeds p_c.

Suspended sediment length scales (L_s) computed from equation (14) vary considerably. Silt-clay L_s values range from 4 km (Good Hope Tributary) to 60 km (Little Conestoga Cr.), while L_s values for sand range from 0.4 km (White Clay Creek) to 113 km (Little Conestoga Cr.).

Table 3. Data Used to Estimate the Mean Age of Mid-Atlantic Eroding Bank Deposits and the Computed Mean Age

Presettlement mean age (yrs)	1761
Presettlement median age (yrs)	615
Presettlement age standard deviation (yrs)	2290
Maximum presettlement age (yrs)	11,240
Minimum presettlement age (yrs)	200
Postsettlement mean age (yrs)	125
Thickness of postsettlement deposits (m)	1.75
Thickness of presettlement deposits (m)	0.5
Thickness weighted mean age (yrs)	488

4.2. Sediment Residence Times

The (nominal) mean age of eroding banks (and hence the value of the sediment storage transit time $\bar{A}_F$) computed using equation (1) is 488 years (Table 3). To obtain this result, 57 C^{14} dates for presettlement deposits (the dates are presented in Table A1 of the supporting information) were averaged. The presettlement C^{14} dates have a mean age of 1761 years, a median age of 615 years, and a maximum age of 11, 240 years.

© 2014. American Geophysical Union. All Rights Reserved.

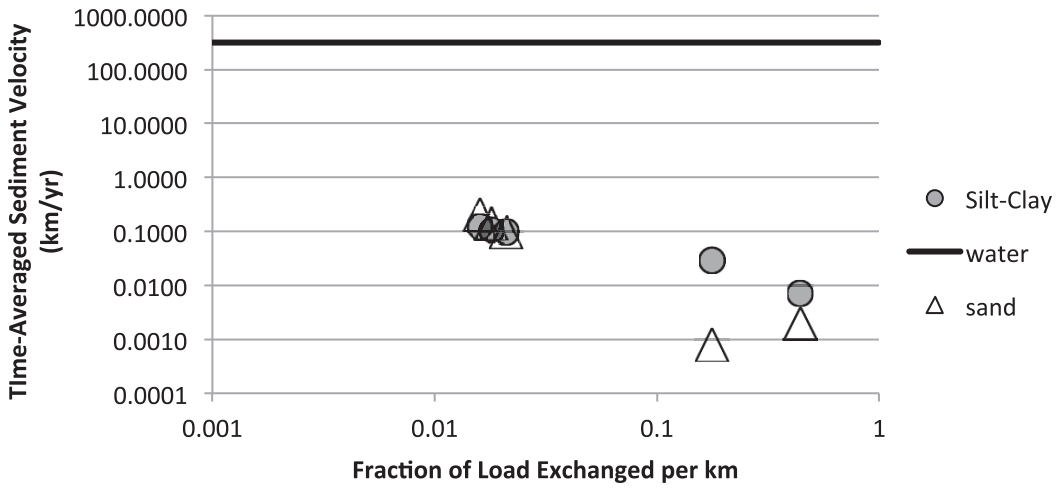

Figure 6. Time-averaged velocities of sediment for the five study sites as a function of the fraction of the suspended sediment load exchanged per km. The velocity of a representative storm flow (1 m/s occurring 1% of the time) is also indicated for comparison (labeled as "water").

4.3. Suspended Sediment Velocities Averaged Over Storage Time Scales

Time-averaged sediment velocities estimated from equation (18) are 3–6 orders of magnitude slower than the representative water velocity (Figure 6), which moves at a rate of 1 m/s occurring 1% of the time (i.e., 315 km/yr). Time-averaged velocities for silt-clay range from 0.0072 km/yr (i.e., 7.2 m/yr) (Good Hope Tributary) to 0.12 km/yr (120 m/yr) (Little Conestoga Cr.) (Table 2), while time-averaged velocities for sand range from 0.0008 km/yr (i.e., 0.8 m/yr) (White Clay Cr.) to 0.20 km/yr (200 m/yr) (Little Conestoga Cr). Surprisingly, time-averaged velocities of sand and silt-clay are approximately equal for the three larger watersheds, with all six velocities on the order of 0.1 km/yr (Figure 6).

5. Discussion

The values of L_s computed with equation (15) and time-averaged velocities computed with equation (19) provide the basis for quantifying the conceptual distance-travel time diagram of Figure 1 (Figure 7) for the five study areas. Results are only presented for silt-clay because these size fractions comprise most of the suspended sediment load. Figure 7 indicates that silt-clay travel times for distances exceeding L_s (i.e., distances greater than ~4–60 km according to Table 2) will likely exceed 10^2 years, and could even be much longer (~1000 years).

A representative value of L_s of 50 km, and other results presented above, provide the basis for developing a quantitative version of the conceptual travel-time diagram of Figure 1 (Figure 8). The travel time for transport within the channel (without storage) increases linearly at a rate of $\hat{U}^{-1}$. For the value of $\hat{U}$ of 315 km/yr used here, this is equivalent to about 10^{-3} yr/km. At this rate, the travel time for a distance $L_s = 50$ km is on the order of 10^{-1} yr. If time in storage is included, travel times increase linearly at a rate of approximately $\bar{A}_F/L_s$ (from equation (22)), or ~10 yr/km, about four orders of magnitude slower than transport in the channel only. At this rate, the travel time for a distance L_s is equal to the storage time A_F, or 488 years. The difference between travel times

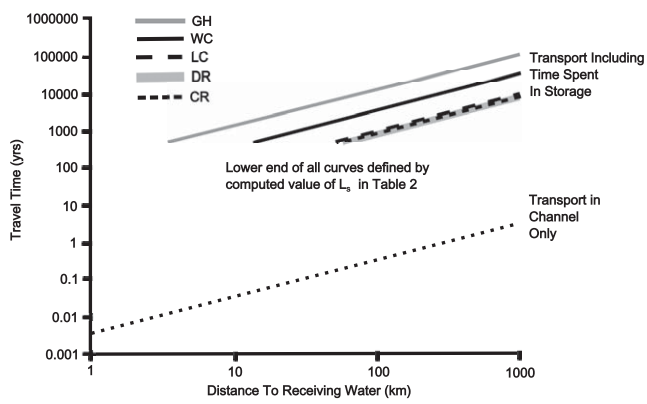

Figure 7. Scaling relations for silt-clay travel time versus distance to receiving waters based on equations (14) and (18).

© 2014. American Geophysical Union. All Rights Reserved.

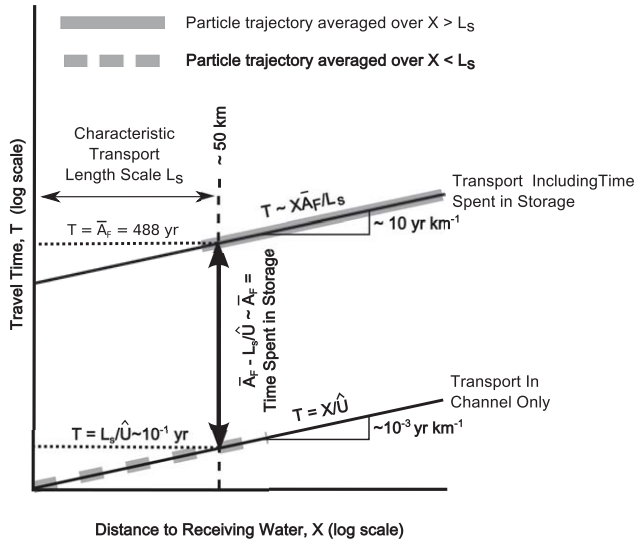

Figure 8. Version of Figure 1 annotated with quantitative estimates. Numerical results assume values of $\hat{U}$ and L_s of 315 km/yr and 50 km, respectively, and $A_F = 488$ yr.

including and neglecting storage (i.e., the vertical separation between the two straight-line trajectories in Figure 8) is $\bar{A}_F - L_s/\hat{U}$, or $\sim\bar{A}_F$ (because $\bar{A}_F$ is ~3 orders of magnitude greater than $L_s/\hat{U}$).

When interpreting Figures 7 and 8, it is important to remember their idealized natures. The theory presented here only considers two sets of length and time scales, one associated with transport in the channel and the other associated with a mean sediment transit time. These two distinct scales are responsible for the "stepped" appearance of particle distance-time trajectories in Figures 1 and 7.

Limiting the analysis to only two scales is useful because both can be parameterized using existing data, one based on simple principles of open channel hydraulics and hydrology and the other from floodplain sediment budgets and geochronology. However, a more realistic approach would necessarily recognize a continuum of length and time scales, as has been well-documented for shorter-term processes that control the downstream movement of dissolved tracers and organic matter in stream channels [*Boano et al.*, 2007; *Haggerty et al.*, 2002; *Harvey et al.*, 2011]. A continuum of length and time scales implies the existence of full distributions of transport length scales and velocities, both of which likely span orders of magnitude. Particle trajectories derived from these distributions would necessarily include much faster and much slower rates of transport to receiving waters than the "representative" mean values illustrated in Figure 7.

Results presented here are further idealized because they neglect the geomorphic architecture of real watersheds. The effects of tributaries and spatial variations in the nature of hydrologic and geomorphic processes have been ignored. For example, stream valleys of the region are typically composed of alternating storage and transport reaches created by underlying geologic structure and unique histories of changing climate, base level, and tectonics [*Hupp et al.*, 2013; *Hack*, 1982]. Figure 7 effectively assumes that watersheds are solely composed of storage reaches; it does not account for the rapid flushing of suspended particles through localized transport reaches such as the bedrock gorges that are often found near the Fall Zone [*Hack*, 1982; *Hupp et al.*, 2013].

Future studies are clearly warranted. For example, a complete numerical solution for the full distribution of C_{Hg} in a real watershed setting should be attempted. This will require specifying the full distribution of particle storage transit times, and should likely include (if only conceptually) other particle storage compartments such as fine-grained channel margin deposits [*Skalak and Pizzuto*, 2010] and the hyporheic zone [*Pizzuto et al.*, 2006]. The spatial structure of the watershed must be resolved, and given the long time scales of particle storage, its geomorphic history as well. Because measurements of sediment budget components are unlikely to cover all locations and historical conditions, process-based theories are needed to predict rates of erosion and deposition, but these must be simple enough to be applied over the scale of large watersheds [e.g., *Pizzuto*, 2012]. Erosional and depositional processes are largely driven by hydrological processes, so a more complete representation of the distribution of storm events and their effects will ultimately be needed [for example, the flow-duration approach followed by *Viparelli et al.*, 2013]. More realistic applications will also have to consider the effects of unbalanced sediment budgets (for example, where deposition might exceed erosion or vice versa), which are common in the mid-Atlantic region [*Hupp et al.*, 2013, *Schenk et al.*, 2013], in addition to historical events that cause sediment budget components to vary with time [*Jacobson and Coleman*, 1986; *Walter and Merritts*, 2008].

© 2014. American Geophysical Union. All Rights Reserved.

Results of model computations, including those presented here, should not be considered equivalent to observational data: they are essentially predictions or hypotheses that require testing. Given the large spatial and temporal scales of watershed particle transport, controlled tracer experiments are impractical. Testing of model predictions will necessarily require exploiting natural isotopic tracers [*Belmont et al*., 2011; *Lauer and Willenbring*, 2010; *Whiting et al*., 2005] and the unintended anthropogenic experiments represented by releases of mine tailings [*Coulthard and Macklin*, 2003; *Lauer and Parker*, 2008b] and heavy metals from industrial processes over known time periods [*Skalak and Pizzuto*, 2010]. The use of isotopic and contaminant tracers is also useful to check results from sediment budgets, which are often notoriously imprecise [*Reid and Dunne*, 2003].

The studies outlined above are needed precisely because the results presented here are probably inadequate to guide watershed restoration planning. While the long particle travel times suggested by Figure 7 imply that BMPs will not be useful if located "far" from receiving waters, a more nuanced view must recognize that the present analysis only applies to "average" particles. Even if Figure 7 correctly represents the mean behavior, the possibility still exists that a significant proportion of the particles in transport will travel faster and farther than average, so even BMPs located far upstream can have some (if somewhat muted) effect on receiving waters in a reasonably short timespan.

6. Conclusions

A simple mass-balance theory is presented that describes the long-term downstream movement of tagged suspended sediment subjected to storage in "off-channel" deposits. The theory requires sediment budget parameters and sediment storage transit times as input. Solution of the equations can in principle document the downstream movement of "tagged" suspended sediment particles through a watershed.

The theory is used to estimate suspended sediment transport length scales and transport velocities for five upland watersheds of the mid-Atlantic region where sediment budget data are available. Transport length scales for silt-clay range from 4 to 60 km, while those for sand range from 0.4 to 113 km. Time-averaged downstream sediment velocities that include time spent in storage are 4–6 orders of magnitude slower than velocities associated with the nominal speed of water movement ($\sim$1 m/s) during a significant storm event that reoccurs 1% of the time. Sediment velocities for silt-clay range from 0.0072 km/yr to 0.12 km/yr, while those of sand range from 0.0008 km/yr to 0.20 km/yr. At two of the sites, velocities of sand movement are much slower than those of silt-clay, while at the other three sites, sand and silt-clay move downstream at approximately equal velocities.

These results suggest that sediment "signals" related to watershed BMPs in upland mid-Atlantic watersheds may take 100–1000 years to reach receiving waters (such as the Chesapeake Bay) if the BMPs are located upstream farther than the characteristic transport length scales. However, the analysis presented here only predicts the mean behavior of a population of suspended particles, and it is likely that some fraction of particles in suspension will travel much faster than average values quoted here. Furthermore, only generalized estimates of particle transit times in storage can be made from the available radiometric dating. Results presented here should be considered preliminary estimates that require verification and elaboration from additional studies.

Acknowledgments
Partial support was provided by NSF grant EAR-0724971. Attribution: J.P. developed the theory, analyzed most of the data, and wrote the first draft of paper; E.R.S., C.R.H., A.G., and G.N. provided data for Difficult Run, Linganore Cr., and Little Conestoga R; E.W. quantified the sediment budget of the White Clay Creek (WCC) with assistance from M.O. in analyzing remotely sensed data; D.K. sampled suspended sediments of the White Clay Cr (WCC) during high flows; J.M. and R.A. performed grain size analysis of suspended sediment data from WCC; D.N. helped interpret gaging station data from the WCC. Chris Sommerfield graciously allowed E.W. to use his Sedigraph for analyzing grain size distribution of floodplain samples from WCC. The manuscript benefited from thoughtful suggestions from Peter Wilcock, Jud Harvey, Sean Smith, and two anonymous reviewers. Any use of trade, product, or firm names is for descriptive purposes only and does not imply endorsement by the U.S. Government.

References

Ackerman, T. R., and J. E. Pizzuto (2012), Partitioning a steady state sediment budget to represent long-tailed distributions of contaminant residence times: A modeling approach for routing tracers through alluvial storage reservoirs, Abstract EP31A-0799 presented at 2012 Fall Meeting, AGU, San Francisco, Calif., 3–7 Dec.

Allmendinger, N. E. (2004), The influence of convex-bank floodplains on stream channel processes and morphology in the mid-Atlantic Piedmont, PhD thesis, 223 pp., Univ. of Delaware, Newark.

Allmendinger, N. E., J. E. Pizzuto, N. Potter, T. E. Johnson, and W. C. Hession (2005), The influence of riparian vegetation on stream width, eastern Pennsylvania, USA, *Geol. Soc. Am. Bull.*, *117*, 229–243, doi:10.1130/B25447.1.

Allmendinger, N. E., J. E. Pizzuto, G. E. Moglen, and M. Lewicki (2007), A sediment budget for an urbanizing watershed, 1951–1996, Montgomery County, Maryland, U.S.A., *J. Am. Water Resour. Assoc.*, *43*, 1483–1498.

Bachman, L. J., B. D. Lindsey, J. W. Brakebill, and D. S. Powars (1998), Ground-water discharge and baseflow nitrate loads of nontidal streams, and their relation to a hydrogeomorphic classification of the Chesapeake Bay watershed, Middle Atlantic coast, *U.S. Geol. Surv. Water Resour. Invest. Rep., 98–4059*, 71 p.

Bain, D. J., and G. S. Brush (2005), Early chromite mining and agricultural clearance: Opportunities for the investigation of agricultural sediment dynamics in the eastern Piedmon (USA), *Am. J. Sci.*, *305*, 957–981.

© 2014. American Geophysical Union. All Rights Reserved.

Belmont, P., et al. (2011), Large shift in source of fine sediment in the Upper Mississippi River, *Environ. Sci. Technol.*, *45*, 8804–8810, doi:10.1021/es2019109.

Boano, F., A. I. Packman, A. Cortis, R. Revelli, and L. Ridolfi (2007), A continuous time random walk approach to the stream transport of solutes, *Water Resour. Res.*, *43*, W10425, doi:10.1029/2007WR006062.

Bolin, B., and H. Rhode (1973), A note on the concepts of age distribution and residence time in natural reservoirs, *Tellus*, *25*, 58–62.

Bradley, D. N., and G. E. Tucker (2013), The storage time, age, and erosion hazard of laterally-accreted sediment on the floodplain of a simulated meandering river, *J. Geophys. Res. Earth Surf.*, *118*, 1308–1319, doi:10.1002/jgrf.20083.

Coulthard, T. J., and M. G. Macklin (2003), Modeling long-term contamination in river systems from historical metal mining, *Geology*, *31*, 451–454.

Crosato, A., and M. S. Saleh (2011), Numerical study on the effects of floodplain vegetation on river planform style, *Earth Surf. Processes Landforms*, *36*, 711–720, doi:10.1002/esp.2088.

Doyle, M. W., and S. H. Ensign (2009), Alternative reference frames in river system science, *Bioscience*, *59*, 499–510.

Ferguson, R. I. (1986), River loads underestimated by rating curves, *Water Resour. Res.*, *22*, 74–76.

Guy, H. P. (1964), An analysis of some storm-period variables affecting stream sediment transport, *U.S. Geol. Surv. Prof. Pap., 464-E*, 50 p.

Hack, J. T. (1982), Physiographic divisions and differential uplift in the Piedmont and Blue Ridge, *U.S. Geol. Surv. Prof. Pap., 1265*, 49 p.

Haggerty, R., W. M. Wondzell, and M. A. Johnson (2002), Power-law residence time distribution in the hyporheic zone of a 2nd-order mountain stream, *Geophys. Res. Lett.*, *29*(13), 1640, doi:10.1029/2002GL014743.

Happ, S. C., G. Rittenhouse, and G. C. Dobson (1940), Some principles of accelerated stream and valley sedimentation, *U.S. Dep. Agric. Tech. Bull.*, *695*, 161 pp.

Harvey, J. W., et al. (2012), Hydrogeomorphology of the hyporheic zone: Stream solute and fine particle interactions with a dynamic streambed, *J. Geophys. Res.*, *117*, G00N11, doi:10.1029/2012JG002043.

Hirsch, R., E. Yagow, M. Ribaudo, K.G. Sellner, J.K. Bohlke, K. Staver, and K. Boomer (2013), Incorporating lag-times into the Chesapeake Bay program, *CRC Pub. 13-004*, 66 pp., STAC, Edgwater, Md. [Available at http://www.chesapeake.org/pubs/305_Hirsch2013.pdf.]

Hupp, C. R., G. B. Noe, E. R. Schenk, and A. J. Benthem (2013), Recent and historic sediment dynamics along Difficult Run, a suburban Virginia Piedmont stream, *Geomorphology*, *180–181*, 156–169, doi:10.1016/j.geomorph.2012.10.007.

Jackson, C. R., G. J. K. Martin, D. S. Leigh, and L. T. West (2005), A southeastern piedmont watershed sediment budget: Evidence for a multimillennial agricultural legacy, *J. Soil Water Conserv.*, *60*, 298–310.

Jacobson, R. B., and D. J. Coleman (1986), Stratigraphy and recent evolution of Maryland Piedmont flood plains, *Am. J. Sci.*, *286*, 617–637.

Kelsey, H. M., R. Lamberson, and M. A. Madej (1987), Stochastic model for the long-term transport of stored sediment in a river channel, *Water Resour. Res.*, *23*, 1738–1750, doi:10.1029/WR023i009p01738.

Lancaster, S. T., and N. E. Casebeer (2007), Sediment storage and evacuation in headwater valleys at the transition between debris-flow and fluvial processes, *Geology*, *35*, 1027–1030, doi:10.1130/G239365A.1.

Lancaster, S. T., E. F. Underwood, and W. T. Frueh (2010), Sediment reservoirs at mountain stream confluences: Dynamics and effects of tributaries dominated by debris-flow and fluvial processes, *Geol. Soc. Am. Bull.*, *122*, 1775–1786, doi:10.1130/B30175.1.

Lauer, J. W., and G. Parker (2008a), Modeling framework for sediment deposition, storage, and evacuation in the floodplain of a meandering river: Theory, *Water Resour. Res.*, *44*, W04425, doi:10.1029/2006WR005528.

Lauer, J. W., and G. Parker (2008b), Modeling framework for sediment deposition, storage, and evacuation in the floodplain of a meandering river: Application to the Clark Fork River, Montana, *Water Resour. Res.*, *44*, W08404, doi:10.1029/2006WR005529.

Lauer, J. W., and G. Parker (2008c), Net local removal of floodplain sediment by river meander migration, *Geomorphology*, *96*, 123–149, doi:10.1016/j.geomorph.2007.08.003.

Lauer, J. W., and J. Willenbring (2010), Steady state reach-scale theory for radioactive tracer concentration in a simple channel/floodplain system, *J. Geophys. Res.*, *115*, F04018, doi:10.1029/2009JF001480.

Lewis, D. W. (1984), *Practical Sedimentology*, 227 pp., Hutchinson Ross, Stroudsburg, Pa.

Malmon, D. V., T. Dunne, and S. L. Reneau (2002), Predicting the fate of sediments and pollutants in river floodplains, *Environ. Sci. Technol.*, *36*, 2026–2032.

Martin, Y., and M. Church (2004), Numerical modeling of landscape evolution: Geomorphological perspectives, *Prog. Phys. Geogr.*, *3*, 317–339.

Meals, D. W., S. A. Dressing, and T. E. Davenport (2010), Lag time in water quality response to best management practices: A review, *J. Environ. Qual.*, *39*, 85–96, doi:10.2134/jeq2009.0108.

Meade, R. H. (2007), Transcontinental moving and storage: The Orinoco and Amazon Rivers transfer the Andes to the Atlantic, in *Large Rivers: Geomorphology and Management*, edited by A. Gupta, pp. 45–64, John Wiley and Sons, Chichester, U. K.

Paola, C., P. L. Heller, and C. L. Angevine (1992), The large-scale dynamics of grain-size variation in alluvial basins, I: Theory, *Basin Res.*, *4*, 73–90.

Parker, G., and Y. Cui (1998), The arrested gravel front: Stable gravel-sand transitions in rivers Part 1: Simplified analytical solution, *J. Hydraul. Res.*, *36*, 75–100.

Pizzuto, J. E. (1987), Sediment diffusion during overbank flows, *Sedimentology*, *34*, 301–317.

Pizzuto, J. E. (2012), Predicting the accumulation of mercury-contaminated sediment on riverbanks—An analytical approach, *Water Resour. Res.*, *48*, W07518, doi:10.1029/2012WR011906.

Pizzuto, J. E., and T. S. Meckelnburg (1989), Evaluation of a linear bank erosion equation, *Water Resour. Res.*, *25*, 1005–1013, doi:10.1029/WR025i005p01005.

Pizzuto, J. E., G. Moglen, M. Palmer, and L. Nelson (2006), Two model scenarios illustrating the effects of land use and climate change on gravel riverbeds of suburban Maryland, U.S.A., in *Gravel-bed Rivers VI—From Process Understanding to River Restoration*, edited by H. Habersack, H. Piegay, and M. Rinaldi, pp. 359–386, Elsevier, Amsterdam.

Reid, L. M., and T. Dunne (2003), Sediment budgets as an organizing framework in fluvial geomorphology, in *Tools in Fluvial Geomorphology*, edited by G. M. Kondolf and H. Piegay, pp. 463–500, John Wiley, Chichester, U. K.

Rhoades, E. L., M. A. O'Neal, and J. E. Pizzuto (2009), Quantifying bank erosion on the South River from 1937–2005, and its importance in assessing Hg contamination, *Appl. Geogr.*, *29*, 125–134.

Schenk, E. R., C. R. Hupp, A. Gellis, and G. Noe (2013), Developing a new stream metric for comparing stream function using a bank-floodplain sediment budget: A case study of three Piedmont streams, *Earth Surf. Processes Landforms*, *38*, 771–784, doi:10.1002/esp.3314.

Skalak, K., and J. Pizzuto (2010), The distribution and residence time of suspended sediment stored within the channel margins of a gravel-bed bedrock river, *Earth Surf. Processes Landforms*, *35*, 435–446, doi:10.1002/esp.1926.

 © 2014. American Geophysical Union. All Rights Reserved.

Smith, S. M. C. (2011), Upland sediment sources in the mid-Atlantic Piedmont, PhD thesis, Dep. of Geogr. and Environ. Eng., Johns Hopkins Univ., Baltimore, Md.

Trimble, S.W. (1971), *Culturally Accelerated Sedimentation on the Middle Georgia Piedmont*, 110 pp., U.S. Soil Conserv. Serv., Fort Worth, Tex.

Viparelli, E., J. W. Lauer, P. Belmont, and G. Parker (2013), A numerical model to develop long-term sediment budgets using isotopic fingerprints, *Comput. Geosci.*, *53*, 114–122, doi:10.1016/j.cageo.2011.10.03.

Walter, R. C., and D. J. Merritts (2008), Natural streams and the legacy of water-powered mills, *Science*, *319*, 299–304.

Warwick, J. J., and R. W. H. Carroll (2008), Evaluating the impacts of uncertainty in geomorphic channel changes on predicting mercury transport and fate in the Carson River System, Nevada, *Int. J. Soil Sediment Water*, *1*, 1–16.

Whiting, P. J., G. Matisoff, W. Fornes, and F. M. Soster (2005), Suspended sediment sources and transport distances in the Yellowstone River basin, *Geol. Soc. Am. Bull.*, *117*, 515–529, doi:10.1130/B25623.1.

Williamson, E. K. (2013), Effect of particle exchange on suspended sediment transport distances in the White Clay Creek, Pennsylvania, MS thesis, Dep. of Geol. Sci., Univ. of Delaware, Newark.

Yorke, T. H., and W. J. Herb (1978), Effects of urbanization on streamflow and sediment transport in the Rock Crek and Anacostia River basins, Montgomery County, Maryland, 1962–1974, *U.S. Geol. Surv. Prof. Pap., 1003*, 71 pp.

© 2014. American Geophysical Union. All Rights Reserved.